Molecular Pharmacology Fast Forward. Published on December 20, 2012 as doi: 10.1124/mol.112.081505

Title Page

5-Cholesten-3β,25-diol 3-sulfate Decreases Lipid Accumulation in Diet-induced Nonalcoholic Fatty Liver Disease Mouse Model

Leyuan Xu, Jin Koung Kim, Qianming Bai, Xin Zhang, Genta Kakiyama, Hae-ki Min, Arun J. Sanyal, William M. Pandak, and Shunlin Ren

Department of Internal Medicine, Virginia Commonwealth University/McGuire Veterans Affairs Medical Center, Richmond, VA, USA: L.X., J.K.K., Q.B., X.Z., G.K., H.K.M., A.J.S., W.M.P., and S.R.

Molecular Pharmacology Fast Forward. Published on December 20, 2012 as DOI: 10.1124/mol.112.081505
This article has not been copyedited and formatted. The final version may differ from this version.

Running Title Page

Running title: 25HC3S decreases serum and hepatic lipids

Address correspondence to: Dr. Shunlin Ren

McGuire Veterans Affairs Medical Center/Virginia Commonwealth University

Research 151, 1201 Broad Rock Blvd, Richmond, VA 23249

E-mail: sren@vcu.edu

Text Pages: 36

Tables: 2

Figures: 6

References: 58

Words in Abstract: 245

Words in Introduction: 750

Words in Discussion: 1328

Abbreviations:

25HC, 25-hydroxycholesterol

25HC3S, 5-cholesten-3β,25-diol 3-sulfate

ABCA(G), ATP-binding cassette, sub-family A(G)

ACC1, acetyl-CoA carboxylase 1

Molecular Pharmacology Fast Forward. Published on December 20, 2012 as DOI: 10.1124/mol.112.081505
This article has not been copyedited and formatted. The final version may differ from this version.

ACOX1, acyl-CoA oxidase 1

CYP7A1, cholesterol 7alpha-hydroxylase

CYP27A1, mitochondrial cholesterol 27alpha-hydroxylase

FAS, fatty acid synthase

GPAM, glycerol-3-phosphate acyltransferase

HFD, high fat diet

HMGR, 3-hydroxy-3-methylglutaryl-CoA reductase

IκBα, nuclear factor of kappa light polypeptide gene enhancer in B-cells inhibitor, alpha

IL, interleukin

LXR, liver X receptor

MCAD, Medium chain acyl-CoA dehydrogenase

NAFLD, nonalcoholic fatty liver disease

NASH, nonaclcoholic steatohepatitis

NFκB, nuclear factor of kappa light polypeptide gene enhancer in B-cells

PLTP, Phospholipid transfer protein

PPAR, peroxisome proliferator-activated receptor

SREBP, sterol regulatory element binding protein

SULT2B1b, sulfotransferase family, cytosolic, 2B, member 1b

TNFα, tumor necrosis factor alpha

Molecular Pharmacology Fast Forward. Published on December 20, 2012 as DOI: 10.1124/mol.112.081505
This article has not been copyedited and formatted. The final version may differ from this version.

Abstract

Background & Aims: Sterol regulatory element binding protein-1c (SREBP-1c) increases lipogenesis at the transcriptional level and its expression is up-regulated by liver X receptor (LXRα). The LXRα/SREBP-1c signaling may play a crucial role in the pathogenesis of nonalcoholic fatty liver disease (NAFLD). We previously reported that a cholesterol metabolite, 5-cholesten-3β,25-diol 3-sulfate (25HC3S), inhibits the LXRα signaling and reduces lipogenesis by decreasing SREBP-1c expression in primary hepatocytes. The present study aims to investigate the effects of 25HC3S on lipid homeostasis in diet-induced NAFLD mouse models. **Methods:** NAFLD was induced by high fat diet (HFD) feeding in C57BL/6J mice. The effects of 25HC3S on the lipid homeostasis, inflammatory responses and insulin sensitivity were evaluated after acute treatments or long-term treatments. **Results:** Acute treatments with 25HC3S decreased serum lipid levels, and long-term treatments decreased hepatic lipid accumulation in the NAFLD mice. Gene expression analysis showed that 25HC3S significantly suppressed the SREBP-1c signaling pathway which was associated with the suppression of the key enzymes involved in lipogenesis: fatty acid synthase (FAS), acetyl-CoA carboxylase (ACC1) and glycerol-3-phosphate acyltransferase (GPAM). In addition, 25HC3S significantly reduced HFD-induced hepatic inflammation as evidenced by decreasing tumor necrosis factor (TNFα) and Interleukin 1 (IL1α/β) mRNA levels. Glucose tolerance test (GTT) and insulin tolerance test (ITT) showed that 25HC3S administration improved HFD-induced insulin resistance. **Conclusion:** The present results indicate that 25HC3S as a potent endogenous regulator decreases lipogenesis, and oxysterol sulfation can be a key protective regulatory pathway against lipid accumulation and lipid-induced inflammation in vivo.

Molecular Pharmacology Fast Forward. Published on December 20, 2012 as DOI: 10.1124/mol.112.081505
This article has not been copyedited and formatted. The final version may differ from this version.

Introduction

Liver plays a pivotal role in maintenance of lipid homeostasis. Accumulation of lipids in liver tissue leads to nonalcoholic fatty liver diseases (NAFLD) (Clark et al., 2002). NAFLD affects 45% of the general population in the USA, with a prevalence of 60-95% in obese patients (Mazza et al., 2012). The spectrum of NAFLD ranges from simple nonprogressive steatosis to progressive nonalcoholic steatohepatitis (NASH) that results in cirrhosis and hepatocellular carcinoma in liver. Hepatocyte lipotoxicity is a key histological feature of NAFLD and is correlated with progressive inflammation and fibrosis (Neuschwander-Tetri, 2010). The hallmark feature of NAFLD is the accumulation of fat in the form of neutral lipid droplets in hepatocytes (Tiniakos et al., 2010). To date, caloric restriction and aerobic exercise are the effective treatments of NAFLD, but they are difficult to achieve for most NAFLD patients. The most promising pharmacological treatment of NAFLD is peroxisome proliferator-activated receptor γ (PPARγ) agonist that decreases lipid accumulation and attenuates inflammatory response in hepatocytes (Ahmed and Byrne, 2007). The results suggest that lowering hepatic lipid levels is a key factor in successful NAFLD therapy. Recently, sterol regulatory element-binding protein-1c (SREBP-1c), has been highly evaluated as a potential target for the treatment of NAFLD, based on its advances to control lipogenic gene expression and regulate fatty acid and triglyceride homeostasis (Ahmed and Byrne, 2007;Goldstein et al., 2006;Horton et al., 2003). Its role in de novo lipogenesis and NAFLD pathogenesis is fully justified (Chen et al., 2004;Grefhorst et al., 2002). Thus, inhibition of hepatic SREBP-1c signaling pathway could improve dyslipidemia and NAFLD.

Oxysterols can act at multiple points in cholesterol homeostasis and lipid metabolism (Gill et al., 2008;Javitt, 2008;van Reyk et al., 2006). Liver oxysterol receptor, LXR, is an oxysterol-regulated

Molecular Pharmacology Fast Forward. Published on December 20, 2012 as DOI: 10.1124/mol.112.081505
This article has not been copyedited and formatted. The final version may differ from this version.

transcription factor in lipid metabolism (Cha and Repa, 2007;Chen et al., 2004). Activation of LXR limits cholesterol synthesis through degradation of 3-hydroxy-3-methylglutaryl-CoA reductase (HMGR) and stimulates cholesterol efflux and clearance through ABCA1 and ABCG5/8. However, activation of LXR upregulates the expression of SREBP-1c, which in turn regulates at least 32 genes involved in lipid biosynthesis and transport (Horton et al., 2002). Therefore, modulation of LXR activation by synthetic ligands could have a profound effect on serum cholesterol levels, but its inappropriate activation of SREBP-1c could lead to hepatic steatosis and hypertriglyceridemia due to the elevated fatty acid and triglyceride synthesis (Grefhorst et al., 2002). Hepatocytes have a limited capacity to store fatty acids in the form of triglycerides, and once overwhelmed, cell damage occurs (Reddy and Rao, 2006).

We have identified an endogenous sulfated oxysterol, 5-cholesten-3β,25-diol 3-sulfate (25HC3S), which accumulates in hepatocyte nuclei after overexpression of mitochondrial cholesterol delivery protein, StarD1 (Ren et al., 2006). 25HC3S is synthesized from 25-hydroxycholesrol (25HC) by sulfotransferase 2B1b, SULT2B1b, via oxysterol sulfation (Li et al., 2007;Fuda et al., 2007;Javitt et al., 2001). Overexpression of SULT2B1b inactivates the response of LXRα triggered by oxysterol and inhibits the expression of LXR target genes including SREBP-1c and ABCA1. The oxysterol sulfation was believed as an inactivation process (Chen et al., 2007). However, overexpression of SULT2B1b or addition of the sulfation product, 25HC3S, into cells decreases both SREBP-1c expression and processing, and suppresses the expression of key enzymes involved in lipid metabolism including acetyl-CoA carboxylase-1 (ACC-1) and fatty acid synthase (FAS). Subsequently, it decreases intracellular neutral lipid and cholesterol accumulation (Bai et al., 2011;Ma et al., 2008;Ren et al., 2007;Xu et al., 2010). These results indicate that oxysterol sulfation and its products may act as a

Molecular Pharmacology Fast Forward. Published on December 20, 2012 as DOI: 10.1124/mol.112.081505
This article has not been copyedited and formatted. The final version may differ from this version.

cholesterol satiety signal that suppresses fatty acid and triglyceride synthesis via inhibition of LXRα/SREBP-1c signaling pathway (Ma et al., 2008). These findings have been further addressed in vivo by overexpression of SULT2B1b in C57BL/6 and LDLR(-/-) mice fed with high fat diet (HFD) or high cholesterol diet (HCD) (Bai et al., 2012). In the presence of 25HC, overexpression of SULT2B1b significantly increases sulfated oxysterols, especially 25HC3S, and thus decreases nuclear LXRα levels and the expression of SREBP-1c, ACC1 and FAS. As a result, overexpression of SULT2B1b in mice reduces lipid levels in sera and lipid accumulation in liver tissues (Bai et al., 2012). Furthermore, 25HC3S increases the expression of cytoplasmic IκBα levels in THP-1 microphages by activation of PPARγ. It reduces LPS-induced IκBα degradation, NFκB nuclear translocation, and the expression and release of TNFα and IL-1β. These results suggest that 25HC3S may act as an endogenous PPARγ ligand that suppresses inflammatory responses via PPARγ/IκB/NFκB signaling pathway. In contrast, 25HC acts in an opposite manner by inducing IκBα degradation and nuclear NFκB accumulations (Xu et al., 2010;Xu et al., 2012). These findings indicate that oxysterol sulfation may also be involved in inflammatory responses and may represent a novel regulatory pathway between lipid homeostasis and inflammatory responses.

In the present study, we demonstrate that acute treatments with 25HC3S substantially decrease serum triglyceride and cholesterol levels, and long-term treatments decrease lipid levels in liver tissues in NAFLD mouse models. LXR/SREBP-1c signaling pathway as a potential molecular mechanism may be involved in 25HC3S administration. These findings provide strong evidence that the oxysterol sulfation product, 25HC3S, acts as a potent regulator involved in lipid metabolism.

Molecular Pharmacology Fast Forward. Published on December 20, 2012 as DOI: 10.1124/mol.112.081505
This article has not been copyedited and formatted. The final version may differ from this version.

Materials and Methods

Chemical synthesis of 5-cholesten-3β, 25-diol 3-sulfate

A mixture of 25-hydroxycholesterol (6.5 mg, 0.016 mmol) and triethylamine-sulfur trioxide (3.5 mg, 0.019 mmol) was dissolved in dry pyridine (300 μl) and was stirred at room temperature for 2 hours. The solvents were evaporated at 40°C under nitrogen stream, and the syrup was added into 100 ml of alkalined CH_3OH, pH 8.0. After the pellets were dissolved completely, the products were filtered and purified by high-performance liquid chromatography (HPLC) using a C18 column with a gradient elution system. A binary system of solvent A (20% CH_3CN in H_2O, v/v) and solvent B (20% CH_3CN in CH_3OH, v/v) was used. It began at 50% A and 50% B with an initial flow rate of 1 ml/min for 10 min and increased to 100% B with an increased flow rate linearly to 2 ml/min over a 30 min period, followed by an additional isocratic period of 20 min. 25HC3S was obtained as its sodium salt (4.7mg, 57%) in white powder. The structure was characterized by mass spectrometry (MS) (**Supplementary Figure 1**) and nuclear magnetic resonance (NMR) spectroscopy analysis (**Supplementary Figure 2**) as previously shown (Harney and Macrides, 2008;Ogawa et al., 2009).

Animal studies

Animal studies were approved by Institutional Animal Care and Use Committee of McGuire Veterans Affairs Medical Center and were conducted in accordance with the Declaration of Helsinki, the Guide for the Care and Use of Laboratory Animals, and all applicable regulations. To examine the effect of 25HC3S on diet-induced lipid accumulation in sera and liver, 8-week-old female C57BL/6J mice (Charles River, Wilmington, MA) were randomly assigned into two groups. The control group was fed with chow diet; and the high fat diet (HFD) group was fed with HFD (Harlan Teklad, Madison, WI) containing 42% kcal from fat, 43% kcal from carbohydrate, 15% kcal from protein and 0.2% cholesterol

Molecular Pharmacology Fast Forward. Published on December 20, 2012 as DOI: 10.1124/mol.112.081505
This article has not been copyedited and formatted. The final version may differ from this version.

for 10 weeks. All mice were housed under identical conditions in an aseptic facility with a 12-hour light/12-hour dark cycle and given free access to water and food. At the end of 10-week period, the mice (n=10-17 in each treatment) were intraperitoneally injected with vehicle solution (ethanol/PBS; Vehicle) or 25HC3S (25 mg/kg) twice and fasted over night (14 hrs) for acute treatments or once every three days for 6 weeks and fasted 5 hrs for long-term treatments. During the long-term treatments, the mice were continually fed with HFD; and their body mass and caloric intake were monitored every week. Blood samples were collected before sacrifice. Serum triglyceride (TG), total cholesterol (CHOL), high density lipoprotein-cholesterol (HDL-C), alkaline phosphatase (ALK), alanine aminotransferase (ALT), and aspartate aminotransferase (AST) were measured using standard enzymatic techniques in the clinical laboratory at McGuire Veterans Affairs Medical Center. Lipoprotein profiles in sera were analyzed by HPLC in the following descriptions.

HPLC analysis of serum lipoprotein profiles

The lipoproteins of triglyceride and cholesterol in very low density lipoprotein (VLDL), low-density lipoprotein (LDL) and high-density lipoprotein (HDL) were measured by gel filtration using HPLC as previously described (Bai et al., 2012). Briefly, mouse serum (100 μl) was eluted with a solvent of 154 mM NaCl with 0.1 mM EDTA (pH 8.0) at a flow rate of 0.2 ml/min via a Pharmacia Superose 6 HR 10/30 FPLC column, and the signal was read at the wavelength of 280 nm. Fractions were collected for 1.2 min each from 20 min up to 100 min. 180 μl of each fraction plus 20 μl of a 10X solution of Wako Total Cholesterol E Reagent (Wako Chemicals USA, Richmond, VA) was incubated in a 96-well plate at 37°C for 3 hrs in dark to analyze cholesterol level, and the absorbance was read at the wavelength of 595 nm. 2 μl of each fraction plus 200 μl of Infinity^{TM} Triglycerides Reagent (Fisher Scientific, Pittsburgh, PA) was incubated in a 96 well plate at 37°C for 5 minutes in dark to analyze

Molecular Pharmacology Fast Forward. Published on December 20, 2012 as DOI: 10.1124/mol.112.081505
This article has not been copyedited and formatted. The final version may differ from this version.

triglyceride level, and the absorbance was read at the wavelength of 500 nm. The lipoprotein profile was monitored as an internal control.

Histo-morphology analysis

Three specimens from different regions of the liver of each mouse were collected and fixed in 4% paraformaldehyde in 0.1 M phosphate buffer at room temperature overnight. The regions of the specimens were standardized for all mice. The paraffin-embedded tissue sections (4 μm) were stained with hematoxylin and eosin (H&E). 3-3'-Diaminobenzidine (DAB) was used as the chromogen, and hematoxylin was used as the nuclear counterstain.

Quantification of hepatic lipids

Liver tissues were homogenized, and the hepatic total lipids were extracted by a mixture of chloroform and methanol (2:1, v:v). After the extracts were filtered, 0.2 ml of each was evaporated to dryness and dissolved in 100 μl of isopropanol containing 10% of triton X-100 for cholesterol assay (Wako Chemicals USA, Richmond, VA), 100 μl of the NEFA solution (0.5 g of EDTA-Na_2, 2 g of Triton X-100, 0.76 ml of 1N NaOH, and 0.5 g of sodium azide/l, pH 6.5) for free fatty acid assay (Wako Chemicals USA, Richmond, VA), or 100 μl of isopropanol only for triglyceride assay (Fisher Scientific, Pittsburgh, PA). All assays were performed according to the manufacturer's instructions, respectively. Each lipid concentration was normalized by liver weight.

Western blot analysis of special protein in cytoplasmic and nuclear extraction

Liver tissues were homogenized, and cytoplasmic and nuclear fractions from liver tissues were extracted by NE-PER Nuclear and Cytoplasmic Extraction Kit (Fisher Scientific, Pittsburgh, PA). The level of

Molecular Pharmacology Fast Forward. Published on December 20, 2012 as DOI: 10.1124/mol.112.081505
This article has not been copyedited and formatted. The final version may differ from this version.

expression of ACC1 (Santa Cruz, sc-30212), FAS (Santa Cruz, sc-55580), SREBP-1 (Santa Cruz, sc-8984) and SREBP-2 (Santa Cruz, sc-5603) were detected by the specific antibodies. β-Actin was used as loading controls for cytoplasmic fractions and Lamin B1 was used as loading controls for nuclear fractions. Each positive band was quantified by Advanced Image Data Analyzer (Aida, Straubenhardt, Germany).

Quantitative real-time polymerase chain reaction (q-RT-PCR) analysis

The relative mRNA levels were measured by real-time reverse transcriptase polymerase chain reaction as previously described (Ren et al., 2004). Briefly, total RNA was isolated with SV Total RNA Isolation Kit (Promega, Madison, WI) that included DNase treatment. 2 μg of total RNA was used in the first-strand cDNA synthesis as recommended by the manufacturer (Invitrogen, Carlsbad, CA). Real-time RT-PCR was performed using SYBR Green as an indicator in ABI 7500 Fast Real-Time PCR System (Applied Biosystems, Foster City, CA). Amplifications of both β-actin and GAPDH were used as internal controls. Relative mRNA expression was quantified with the comparative cycle threshold (Ct) method and expressed as $2^{-\Delta\Delta Ct}$. The sequences of primers were obtained from http://www.pga.mgh.harvard.edu/primerbank/ and summarized in **Supplementary Table 1**.

Insulin sensitivity analysis

Glucose tolerance tests were performed by an intraperitoneal injection of D-glucose (Sigma-Aldrich Corporation, St. Louis, MD) at a dose of 2 g/kg of body weight after an overnight (12 hrs) fasting. Insulin tolerance tests were performed by an intraperitoneal injection of insulin (Novolin R, Novo Nordisk Inc., Princeton, NJ) at a dose of 0.5 U/kg of body weight after a 4 hrs fasting. Blood samples were collected via the tail vein, and plasma glucose was monitored by Precision Xtra Blood Glucose

Molecular Pharmacology Fast Forward. Published on December 20, 2012 as DOI: 10.1124/mol.112.081505
This article has not been copyedited and formatted. The final version may differ from this version.

Monitoring System (Abbott Diabetes Care Inc., Alameda, CA).

Analysis of hepatic oxysterols and oxysterol sulfates by HPLC

Mouse liver samples (400 mg) were digested by 2 mg/ml of proteinase K in PBS (1ml) at 50°C for 12 hours, and 40ml of chloroform:methanol (2:1, v:v) was added to the digests. The mixture was sonicated for 30 min and filtered to remove insoluble materials. Then, 6 ml of water with 100 μl of 1 M K_2CO_3 was added into the mixture and shaken well before allowing it to stand for about 3 hours for phase separation.

The water/methanol phase that mainly contained sulfated oxysterols was evaporated under N_2. The residues were re-suspended in 20% methanol by sonication and passed through a Sep-Pak tC18 cartridge (Waters, Milford, MA). After the cartridge was washed by 20% methanol for three times, the sulfated oxysterol fractions were eluted by 60% methanol and taken to dryness under N_2 stream below 40°C. The extracts were then solvolyzed in a mixture of acetone (1 ml), methanol (9 ml), and conc. HCl (20 μl) at 39°C overnight. After the mixture was neutralized by 5% KOH in methanol, 30 μl of testosterone in chloroform solution (50 μg/ml) was added, and the whole mixture was evaporated to dryness. The residues were re-suspended in 8ml of hexane and loaded into a Waters Sep-Pak silica cartridge (400 mg) that had been pre-washed by 2% isopropanol in hexane. The purified oxysterols fractions were finally eluted by 8 ml of isopropanol:hexane (1:9, v/v) and evaporated under N_2.

The chloroform phase that mainly contains non-sulfated oxysterols was added 30 μl of testosterone in chloroform solution (50 μg/ml) and evaporated under N_2 below 40°C. The residue was re-suspended in 8 ml of hexane and passed through a Waters Sep-Pak silica cartridge to purify the oxysterol fraction

Molecular Pharmacology Fast Forward. Published on December 20, 2012 as DOI: 10.1124/mol.112.081505
This article has not been copyedited and formatted. The final version may differ from this version.

as described above.

Both methanol/water phase and chloroform phase hereby containing the oxysterols were derivatized to the corresponding 3-Keto-Δ^4 form with cholesterol oxidase essentially according to the reported method (Zhang et al., 2001), and they were analyzed by Water Alliance series 2695 HPLC module fitted with 2487 Dual λ absorbance detector (Waters, Milford, MA). The separation was carried out by an eluent of hexane:isopropanol:acetic acid (965:25:10, v:v:v) at a flow rate of 1.3ml/min through an Ultraspere silica column (5 μm, 4.6 mm *id* x 250 mm; Beckman, Urbana, IL). The column temperature was kept constant at 30°C and the enones were monitored at the absorption at 240 nm.

Statistical Analysis

All results were expressed as means ± standard errors. Western blot results were repeated at least three times. Statistical analysis was performed with Student *t*-test for unpaired samples. A value of $p < 0.05$ was considered as statistically significant.

Molecular Pharmacology Fast Forward. Published on December 20, 2012 as DOI: 10.1124/mol.112.081505
This article has not been copyedited and formatted. The final version may differ from this version.

Results

25HC3S administration reduces serum lipid levels in mice fed a HFD.

25HC3S has been shown to reduce lipid accumulation in both primary hepatocytes and THP-1 macrophages (Ma et al., 2008;Ren et al., 2007;Xu et al., 2010). To investigate the effects of 25HC3S on hyperlipidemia in vivo, 8-week-old C57BL/6J female mice were fed with HFD to establish a NAFLD model, and mice were fed with chow diet as a negative control. After 10 weeks of feeding, the mice were treated with 25HC3S or vehicle twice in 14 hrs and fasted overnight as acute treatments. Caloric intake and weight gain were similar in both treated groups. As expected, 10 weeks of feeding with HFD significantly elevated plasma TG, CHOL, and HDL-C by 1.4-fold, 1.9-fold and 1.8-fold, respectively. In HFD group, compared to the vehicle treatments, the acute treatments with 25HC3S significantly decreased plasma TG, CHOL, and HDL-C by 40%, 15% and 20%, respectively (**Figure 1A-C**). Plasma triglyceride level was reduced to the same level as in chow diet-fed healthy mice (**Figure 1A**). Liver function analysis showed that HFD raised serum ALT and AST levels, but there was no significant difference between 25HC3S-treated and vehicle-treated mice (**data not shown**), indicating acute administration of 25HC3S had no effect on liver function.

The serum lipid profiles were further confirmed by HPLC analysis. Acute treatments with 25HC3S did not change LDL, VLDL, and HDL protein levels (**Figure 1D**) but markedly decreased triglyceride contents in VLDL fractions and slightly decreased cholesterol contents in HDL fractions (**Figure 1E-F**), that is consistent with enzymatic analysis (**Figure 1A-C**). These results indicate that acute administration of 25HC3S significantly lowers serum lipid levels in the circulation in NAFLD mouse model.

Molecular Pharmacology Fast Forward. Published on December 20, 2012 as DOI: 10.1124/mol.112.081505
This article has not been copyedited and formatted. The final version may differ from this version.

Analysis of 25HC3S in liver tissues

To study the effects of 25HC3S on hepatic lipid metabolism in the mice fed with HFD, the concentration of 25HC3S in the liver tissues from treated mice was determined by HPLC analysis. The results indicated that acute treatments of 25HC3S significantly increased its accumulation in liver (**Figure 2**). It was observed that a small peak of 25HC presented in 25HC3S-treated mice liver (**Figure 2**), indicating that a small amount of 25HC3S was degraded to 25HC, where steroid sulfatase (STS) may be involved (Snyder et al., 2000).

Hepatic mRNA expression in the 25HC3S-treated mice

To compare the regulation of lipogenic gene expression in response to acute treatments of 25HC3S in liver, we determined the mRNA expression by real time RT-PCR as shown in **Table. 1**. Acute treatments of 25HC3S significantly suppressed the expression of the genes involved in fatty acid biosynthesis. Compared to vehicle-treated mice liver, 25HC3S reduced the mRNA levels of SREBP-1c, ACC1 and FAS by 46%, 57%, and 49%, respectively, which were consistent with previous in vitro results (Ren et al., 2007;Xu et al., 2010). However, there was no significant difference on the mRNA levels of PPARα, CPT1, ACOX1, MCAD and SCAD between 25HC3S- and vehicle-treatment (**Table. 1**). These results suggest that acute administration of 25HC3S lowers serum TG by inhibition of fatty acid synthesis but not stimulation of its oxidation. In addition, 25HC3S significantly suppressed ABCA1 expression, which may explain the lower level of plasma HDL cholesterol (**Figure 1C, F**).

25HC3S administration decreases nuclear SREBP-1 protein levels and cytoplasmic FAS and ACC1 protein level in liver tissues.

Molecular Pharmacology Fast Forward. Published on December 20, 2012 as DOI: 10.1124/mol.112.081505
This article has not been copyedited and formatted. The final version may differ from this version.

SREBP-1c up-regulates fatty acid and triglyceride biosynthesis by binding with SREBP-1 response elements and increasing expression of rate-limiting enzymes including FAS and ACC1. To determine if 25HC3S inactivated the SREBP-1c pathway, nuclear SREBP-1 protein levels in liver tissues were determined by Western blot analysis. Interestingly, HFD feeding markedly increased nuclear SREBP-1 mature form and induced its target gene ACC1 expression (**data not shown**). 25HC3S significantly suppressed nuclear SREBP-1, cytoplasmic ACC1 and FAS protein levels by 74%, 58% and 47%, respectively (**Figure 3**), which is consistent with mRNA levels as shown in (**Table. 1**). These results suggest that acute administration of 25HC3S suppresses lipogenesis by inhibition of SREBP-1c signaling pathway.

Effects of long-term treatments of 25HC3S on lipid homeostasis in HFD-fed mice

To study effects of long-term treatments of 25HC3S on lipid homeostasis, 8-week-old C57BL/6J female mice were fed with HFD for 10 weeks, and then, they were divided into two groups. One was treated with 25HC3S by peritoneal injection once every three days for 6 weeks, and the other one was treated with vehicle in the same conditions. During the treatments, the mice were continuously fed with HFD. The body mass and caloric intakes were monitored every week. The body mass of 25HC3S-treated mice increases significantly slower than the control mice, but there is no significant difference in the caloric intake between these two groups (**Figure 4A-B**). After 6 weeks injection, the mice were fasted for 5 hrs before sacrifice. The average liver weight was significantly decreased in 25HC3S-treated group (**Figure 4C**).

As expected, 25HC3S significantly decreased plasma cholesterol level as compared to vehicle-treated mice, but surprisingly, 25HC3S did not significantly decrease plasma TG level (**data not shown**). The

Molecular Pharmacology Fast Forward. Published on December 20, 2012 as DOI: 10.1124/mol.112.081505
This article has not been copyedited and formatted. The final version may differ from this version.

liver function analysis indicated that 25HC3S treatment significantly reduced serum ALK, ALT and AST levels (**Figure 4D-F**). These results indicate that 25HC3S treatment protects the liver from injury that may be through suppressing hepatic inflammation.

To study the effect of 25HC3S on hepatic lipid metabolism, we measured hepatic lipid level and gene expression. As expected, HFD feeding in mice significantly increased triglyceride, total cholesterol, free cholesterol, and free fatty acid levels in liver by 3-, 3.5- 3.2- and 2.5-fold compared to chow diet feeding ($p < 0.01$). However, long-term treatments of 25HC3S significantly reduced these levels by 30%, 15%, 28% and 23%, respectively (**Figure 5A-D**). It was noticed that cholesterol ester concentration was not affected by the administration of 25HC3S (**Figure 5E**). The decreases in lipid levels were further confirmed by morphological analysis (**Figure 5F**). The liver from the mice fed with HFD was pale and was distended by large cytoplasmic lipid inclusions compared to the liver from the mice fed with chow diet, suggesting NAFLD model was successfully established following HFD feeding. Long-term treatments with 25HC3S significantly decreased lipid inclusions in hepatocytes.

Gene expression analysis showed that long-term treatments with 25HC3S significantly decreased mRNA levels of SREBP-1c, ACC1 and FAS by 23%, 41%, and 27%, respectively (**Table 2**), which is consistent with the acute treatments (**Table. 1**). More interestingly, long-term treatments with 25HC3S significantly decreased the expression of the key enzymes involved in triglyceride synthesis, GPAM, by 21%, as well as lipid transfer protein, MTTP and PLTP by 23% and 39%, respectively. In addition, long-term treatments with 25HC3S decreased the expression of the genes involved in oxidized LDL uptake, CD36 and SRB1, by 48% and 21%, respectively. Both genes are known to contribute to the development of foam cells (Abumrad and Davidson, 2012), but CD36 is also known to be involved in

Molecular Pharmacology Fast Forward. Published on December 20, 2012 as DOI: 10.1124/mol.112.081505
This article has not been copyedited and formatted. The final version may differ from this version.

hepatic inflammation (Li et al., 2012;Bieghs et al., 2012).

Dysregulation of lipid metabolism is frequently associated with inflammatory conditions. Elevated circulating FFA may be directly cytotoxic to the liver by stimulating TNFα expression via a lysosomal pathway; activating mitogen-activated protein kinase cascades and oxidative stress (Feldstein et al., 2004;Malhi et al., 2006). Thus, it was of interest to investigate the effect of 25HC3S on hepatic inflammatory response. Long-term treatments of 25HC3S significantly suppressed the mRNA expression of pro-inflammatory cytokines, TNFα, IL1α, and IL1β, by 47%, 48%, and 50%, respectively (**Table. 2**). The similar effect has been observed in the acute treatments of 25HC3S, where the mRNA expression of TNFα was decreased by 35% (**Table. 1**). These results are consistent with liver function assay that 25HC3S suppresses liver inflammatory responses and prevents liver damage (**Figure 4E-F**).

Under condition of metabolic disorders, lipid accumulation in the liver is always associated with the development of insulin resistance. As reported, HFD feeding significantly elevated fasting glucose and insulin levels in mice compared with chow diet feeding (Li et al., 2010). To study the effect of 25HC3S on glucose homeostasis and insulin sensitivity, glucose tolerance test (GTT) and insulin tolerance test (ITT) were performed after long-term treatments of 25HC3S. As shown in **Figure 6A**, administration of 25HC3S significantly decreased fasting glucose levels and improved insulin sensitivity (**Figure 6B**), suggesting that repression of lipid accumulation in liver and circulation by 25HC3S administration improves glucose homeostasis and insulin sensitivity in HFD-fed mice.

Molecular Pharmacology Fast Forward. Published on December 20, 2012 as DOI: 10.1124/mol.112.081505
This article has not been copyedited and formatted. The final version may differ from this version.

Discussion

The liver is a key metabolic organ in response to the imbalance of high-caloric diets, especially HFD, and it plays a central role in lipid homeostasis (Canbay et al., 2007). Due to HFD consumption or obesity, plasma FFA levels are elevated, which induces intrahepatocellular accumulation of triglycerides and diacylglycerol and produces low-grade inflammation in liver through activation of NFκB, resulting in release of several proinflammatory cytokines, such as IL-6. Lipotoxicity induced by elevated FFA increases oxidative stress and causes insulin resistance in muscle, liver and endothelial cells. Excess FFA contributes to the accumulation of lipid droplets in hepatocytes, which becomes the hallmark of liver diseases such as dyslipidemia, NAFLD, hypertension and type 2 diabetes mellitus (Boden, 2006;Malhi and Gores, 2008). The pathogenesis of NAFLD is complex, but the transcription factors of hepatic lipid and glucose homeostasis may be a key to treat NAFLD. As a key transcription factor regulating hepatic fatty acid and triglyceride synthesis, SREBP-1c activity modulation has been evaluated as a potential new treatment for NAFLD (Ahmed and Byrne, 2007;Vallim and Salter, 2010).

LXRs are members of the nuclear receptor superfamily of ligand-activated transcriptional factors involved in the regulation of lipid metabolism and inflammatory process (Torocsik et al., 2009). Administration of LXR agonist to mice induces a mild and transient hypertriglyceridemia and hepatic steatosis. The molecular mechanism for this is that LXRs activate triglyceride synthesis in liver directly and indirectly by inducing SREBP-1c expression (Chen et al., 2004;Okazaki et al., 2010). In our previous studies, we identified a cholesterol metabolite, 25HC3S, in primary hepatocytes overexpressing StARD1 (Li et al., 2007;Ren et al., 2006). When intracellular cholesterol levels are increased, StARD1 delivers cholesterol into mitochondria where regulatory oxysterols, such as 25HC, are synthesized by CYP27a1 (Li et al., 2006;Li et al., 2007). These oxysterols can activate LXRα and

Molecular Pharmacology Fast Forward. Published on December 20, 2012 as DOI: 10.1124/mol.112.081505
This article has not been copyedited and formatted. The final version may differ from this version.

then upregulate the expression of SREBP-1c, which induces hepatic lipogenesis (Ferber, 2000;Gill et al., 2008). 25HC can further be sulfated in the cytoplasm by SULT2B1b to 25HC3S when delivery of cholesterol to the mitochondria is increased (Ren et al., 2006;Li et al., 2007). 25HC3S in turn inactivates LXRα, suppresses SREBP-1c expression, and subsequently decreases intracellular lipid levels (Ma et al., 2008;Ren et al., 2007;Xu et al., 2010). In our recent report, in vivo, overexpression of SULT2B1b significantly increased 25HC3S formation in liver and lowered lipid levels in the serum and in the liver by inhibition of LXRα/SREBP-1c signaling pathway in mice fed with HFD. This was observed only in the presence of 25HC, but not in the absence of 25HC. The same effects were also observed in LDLR knockout mice, indicating that SULT2B1b reduced serum and hepatic lipid levels due to the suppression of lipid biosynthesis rather than clearance.

In the current study, we provide the first evidence for the effect of 25HC3S on HFD-induced NAFLD models in vivo. 25HC3S not only reduced HFD-induced lipid accumulation in serum and liver, but also suppressed HFD-induced hepatic inflammation and insulin resistance. Since several mechanisms could account for the protective effect of 25HC3S in this model, to seek an explanation, we analyzed the expression of different genes involved in fatty acid synthesis, fatty acid β-oxidation, triglyceride synthesis, cholesterol metabolism and lipid clearance. Interestingly, administration of 25HC3S to the mice significantly suppressed fatty acid synthesis by suppressing SREBP-1c, ACC1 and FAS expression, but led little effect on fatty acid β-oxidation (**Tables 1, 2**). As reported, HFD feeding markedly induces the expression of SREBP-1 in wild-type mice (Li et al., 2010). Four SREBP-1c target genes, ACC1, FAS, GPAM and PLTP, have been identified following administration of LXR agonist, T0901317, to wild-type, LRLR-/- and LDLR-/-, SREBP-1c-/- mice (Okazaki et al., 2010). Among these, the most likely candidate genes involved in fatty acid and triglyceride synthesis are ACC1, FAS

Molecular Pharmacology Fast Forward. Published on December 20, 2012 as DOI: 10.1124/mol.112.081505
This article has not been copyedited and formatted. The final version may differ from this version.

and GPAM. PLTP has been found to increase hepatic VLDL secretion (Jiang et al., 2001). Together, HFD activates LXR/SREBP-1c signaling pathway and increases large VLDL particles via two processes. One is the increase of triglyceride production by activation of fatty acid and triglyceride biosynthesis, and the other is the increase of triglyceride loading in VLDL particles by upregulation of PLTP to insert additional phospholipids into the particles (Okazaki et al., 2010). Our current data in mice suggests that the reduction of serum triglyceride (**Figure 1A**), especially in VLDL particles (**Figure 1E**), by administration of 25HC3S may be due to both processes: the decrease of lipogenesis by suppression of ACC1, FAS and GPAM (**Tables 1, 2**), as well as the decrease of VLDL particle assembly by suppression of PLTP (**Table 2**). These results indicate the inhibition of LXR/SREBP-1c signaling pathway may be involved in 25HC3S-treated mice. Besides, ABCA1, ABCG1, ABCG5 and CYP7α have been reported as the other LXR targets involved in cholesterol clearance (Ando et al., 2005;Baldan et al., 2009;Li et al., 2010). Our current data shows the administration of 25HC3S in mice suppressed the mRNA expression of ABCA1, ABCG1 and CYP7α and led a decrease in cholesterol efflux (**Tables 1, 2**). As a result, 25HC3S treatment in mice reduced cholesterol levels in HDL particles (**Figure 1C-F**). In our previous report, 25HC3S inhibits the LXRE-luciferase reporter gene expression induced by 25HC or LXR agonist T0901317 in H441 cells transfected with either LXRα or LXRβ recombinant plasmid (Ma et al., 2008). However, LXRα and LXRβ have overlapping but discrete functions. LXRβ has been reported as a major regulator of glucose homeogenesis, energy utilization, and fat storage in muscle and white adipose tissue (Korach-Andre et al., 2010;Polyzos et al., 2012). The present data further supports that 25HC3S serves as an endogenous LXR antagonist, suppressing LXR target gene expression in vivo.

The progression of NAFLD to NASH is characterized by hepatocyte lipotoxicity. Several studies have

Molecular Pharmacology Fast Forward. Published on December 20, 2012 as DOI: 10.1124/mol.112.081505
This article has not been copyedited and formatted. The final version may differ from this version.

demonstrated a major contribution of pro-inflammatory cytokines, such as TNFα, IL-1 and IL-6, to the progression from steatosis to steatohepatitis (Neuschwander-Tetri, 2010;Tilg and Moschen, 2010). Levels of these pro-inflammatory cytokines correlate with the stage of fibrosis and with the NAFLD activity score in NASH (Manco et al., 2007). In our previous report, 25HC3S significantly suppresses TNFα induced inflammatory response in HepG2 cells and LPS induced inflammatory response in THP-1 microphages (Xu et al., 2010;Xu et al., 2012). Addition of 25HC3S to human macrophages markedly increased nuclear PPARγ, cytosol IκB, and decreased nuclear NFκB protein levels. 25HC3S significantly increased PPARγ-luciferase report gene expression. The Ki for 25HC3S was ~1 μM similar to other PPARγ ligands in PPARγ-competitor assay suggesting this effect is via PPARγ/IκBα signaling pathway (Xu et al., 2012). In the present study, we also observed that administration of 25HC3S to the mice significantly suppressed hepatic mRNA expression of TNFα (**Tables 1, 2**) and IL-1α/β (**Table 2**). Subsequently, it reduced liver damage by the decrease of serum ALT and AST levels (**Figure 4E-F**). Interestingly, we didn't observe a significant increase in the mRNA expression of IκBα in liver by 25HC3S administration as we previously showed in vitro (Xu et al., 2010).

Due to the excess FFA, the development of NAFLD and NASH not only causes ectopic fat accumulation in liver, but also raises insulin resistance in adipose tissue (Cusi, 2012;Samuel and Shulman, 2012). Our preliminary studies suggest that the suppression of lipogenesis by 25HC3S administration in mice leads a decrease in ectopic lipid droplets accumulation in hepatocytes (**Figure 5**). Ultimately, it led to improved insulin signaling and reduced insulin resistance (**Figure 6**).

Dietary cholesterol such as HFD or high cholesterol diet induces hepatic cholesterol ester and triglyceride accumulation in liver tissues. The excess cholesterol will be metabolized to oxysterols

Molecular Pharmacology Fast Forward. Published on December 20, 2012 as DOI: 10.1124/mol.112.081505
This article has not been copyedited and formatted. The final version may differ from this version.

such as 25HC, 27HC and 24-(S), 25-epoxycholesterol (24,25-EC) and in turn to activate LXR (Basciano et al., 2009). These oxysterols may be surrogate markers of insulin resistance, and the high oxysterol levels in the circulation play an important role in the development of hepatic and peripheral insulin resistance followed by NAFLD (Ikegami et al., 2012). The present study shows that 25HC3S as a potent endogenous regulator has a beneficial effect on dyslipidemia and early stage of NAFLD, and oxysterol sulfation is another novel systematic regulatory pathway involved in regulating lipid and glucose homeostasis and inflammatory response. These results indicate that 25HC3S decreases lipogenesis by inhibiting the SREBP-1c signaling pathway in vivo. Oxysterol sulfation can be a key protective regulatory pathway against lipid accumulation and lipid-induced inflammation in liver (Cha and Kim, 2012;Polyzos et al., 2012). There are 48 and 49 nuclear receptors identified in humans and mice, respectively, including classical steroid hormone receptors, orphan receptors and adopted orphan receptors. Many of them are involved in lipid metabolism, and their ligands are believed to be lipid derivatives. Current results indicate that 25HC3S decreases lipogenesis most likely via inhibiting LXRα/SREBP-1c signaling pathway in vivo. However, the detailed mechanism of molecular-molecular interaction needs further investigation.

Molecular Pharmacology Fast Forward. Published on December 20, 2012 as DOI: 10.1124/mol.112.081505
This article has not been copyedited and formatted. The final version may differ from this version.

Acknowledgement

We acknowledge excellent technical help from Patricia Cooper, Dalila Marques, and Kaye Redford.

Molecular Pharmacology Fast Forward. Published on December 20, 2012 as DOI: 10.1124/mol.112.081505
This article has not been copyedited and formatted. The final version may differ from this version.

Author Contributions

Participated in research design: Leyuan Xu and Shunlin Ren

Conducted experiments: Leyuan Xu, Jin Koung Kim, Qianming Bai, Xin Zhang, and Genta Kakiyama

Contributed new reagents: Leyuan Xu and Genta Kakiyama

Performed data analysis: Leyuan Xu and Shunlin Ren

Wrote or contributed to the writing of the manuscript: Leyuan Xu, Hae-ki Min, Arun J. Sanyal, William M. Pandak, and Shunlin Ren

Molecular Pharmacology Fast Forward. Published on December 20, 2012 as DOI: 10.1124/mol.112.081505
This article has not been copyedited and formatted. The final version may differ from this version.

Reference List

Abumrad NA and Davidson N O (2012) Role of the Gut in Lipid Homeostasis. *Physiol Rev* **92**:1061-1085.

Ahmed MH and Byrne C D (2007) Modulation of Sterol Regulatory Element Binding Proteins (SREBPs) As Potential Treatments for Non-Alcoholic Fatty Liver Disease (NAFLD). *Drug Discov Today* **12**:740-747.

Ando H, Tsuruoka S, Yamamoto H, Takamura T, Kaneko S and Fujimura A (2005) Regulation of Cholesterol 7alpha-Hydroxylase MRNA Expression in C57BL/6 Mice Fed an Atherogenic Diet. *Atherosclerosis* **178**:265-269.

Bai Q, Xu L, Kakiyama G, Runge-Morris M A, Hylemon P B, Yin L, Pandak W M and Ren S (2011) Sulfation of 25-Hydroxycholesterol by SULT2B1b Decreases Cellular Lipids Via the LXR/SREBP-1c Signaling Pathway in Human Aortic Endothelial Cells. *Atherosclerosis* **214**:350-356.

Bai Q, Zhang X, Xu L, Kakiyama G, Heuman D, Sanyal A, Pandak W M, Yin L, Xie W and Ren S (2012) Oxysterol Sulfation by Cytosolic Sulfotransferase Suppresses Liver X Receptor/Sterol Regulatory Element Binding Protein-1c Signaling Pathway and Reduces Serum and Hepatic Lipids in Mouse Models of Nonalcoholic Fatty Liver Disease. *Metabolism* **61**:836-845.

Baldan A, Bojanic D D and Edwards P A (2009) The ABCs of Sterol Transport. *J Lipid Res* **50 Suppl**:S80-S85.

Basciano H, Miller A E, Naples M, Baker C, Kohen R, Xu E, Su Q, Allister E M, Wheeler M B and Adeli K (2009) Metabolic Effects of Dietary Cholesterol in an Animal Model of Insulin Resistance and Hepatic Steatosis. *Am J Physiol Endocrinol Metab* **297**:E462-E473.

Bieghs V, van Gorp P J, Walenbergh S M, Gijbels M J, Verheyen F, Buurman W A, Briles D E, Hofker M H, Binder C J and Shiri-Sverdlov R (2012) Specific Immunization Strategies Against Oxidized Low-Density Lipoprotein: A Novel Way to Reduce Nonalcoholic Steatohepatitis in Mice. *Hepatology* **56**:894-903.

Boden G (2006) Fatty Acid-Induced Inflammation and Insulin Resistance in Skeletal Muscle and Liver. *Curr Diab Rep* **6**:177-181.

Canbay A, Bechmann L and Gerken G (2007) Lipid Metabolism in the Liver. *Z Gastroenterol* **45**:35-41.

Cha JY and Kim Y B (2012) Sulfated Oxysterol 25HC3S As a Therapeutic Target of Non-Alcoholic Fatty Liver Disease. *Metabolism.*

Cha JY and Repa J J (2007) The Liver X Receptor (LXR) and Hepatic Lipogenesis. The Carbohydrate-Response Element-Binding Protein Is a Target Gene of LXR. *J Biol Chem* **282**:743-751.

Chen G, Liang G, Ou J, Goldstein J L and Brown M S (2004) Central Role for Liver X Receptor in Insulin-Mediated Activation of Srebp-1c Transcription and Stimulation of Fatty Acid Synthesis in Liver. *Proc Natl Acad Sci U S A* **101**:11245-11250.

Chen W, Chen G, Head D L, Mangelsdorf D J and Russell D W (2007) Enzymatic Reduction of Oxysterols Impairs LXR Signaling in Cultured Cells and the Livers of Mice. *Cell Metab* **5**:73-79.

Clark JM, Brancati F L and Diehl A M (2002) Nonalcoholic Fatty Liver Disease. *Gastroenterology* **122**:1649-1657.

Cusi K (2012) Role of Obesity and Lipotoxicity in the Development of Nonalcoholic Steatohepatitis: Pathophysiology and Clinical Implications. *Gastroenterology* **142**:711-725.

Feldstein AE, Werneburg N W, Canbay A, Guicciardi M E, Bronk S F, Rydzewski R, Burgart L J and Gores G J (2004) Free Fatty Acids Promote Hepatic Lipotoxicity by Stimulating TNF-Alpha Expression Via a Lysosomal Pathway. *Hepatology* **40**:185-194.

Ferber D (2000) Lipid Research. Possible New Way to Lower Cholesterol. *Science* **289**:1446-1447.

Fuda H, Javitt N B, Mitamura K, Ikegawa S and Strott C A (2007) Oxysterols Are Substrates for Cholesterol Sulfotransferase. *J Lipid Res* **48**:1343-1352.

Gill S, Chow R and Brown A J (2008) Sterol Regulators of Cholesterol Homeostasis and Beyond: the Oxysterol Hypothesis Revisited and Revised. *Prog Lipid Res* **47**:391-404.

Goldstein JL, DeBose-Boyd R A and Brown M S (2006) Protein Sensors for Membrane Sterols. *Cell* **124**:35-46.

Grefhorst A, Elzinga B M, Voshol P J, Plosch T, Kok T, Bloks V W, van der Sluijs F H, Havekes L M, Romijn J A, Verkade H J and Kuipers F (2002) Stimulation of Lipogenesis by Pharmacological Activation of the Liver X Receptor Leads to Production of Large, Triglyceride-Rich Very Low Density Lipoprotein Particles. *J Biol Chem* **277**:34182-34190.

Harney DW and Macrides T A (2008) Synthesis of an Isomeric Mixture (24RS,25RS) of Sodium Scymnol Sulfate. *Steroids* **73**:424-429.

Horton JD, Goldstein J L and Brown M S (2002) SREBPs: Activators of the Complete Program of Cholesterol and Fatty Acid Synthesis in the Liver. *J Clin Invest* **109**:1125-1131.

Horton JD, Shah N A, Warrington J A, Anderson N N, Park S W, Brown M S and Goldstein J L (2003) Combined Analysis of Oligonucleotide Microarray Data From Transgenic and Knockout Mice Identifies Direct SREBP Target Genes. *Proc Natl Acad Sci U S A* **100**:12027-12032.

Ikegami T, Hyogo H, Honda A, Miyazaki T, Tokushige K, Hashimoto E, Inui K, Matsuzaki Y and Tazuma S (2012) Increased Serum Liver X Receptor Ligand Oxysterols in Patients With Non-Alcoholic Fatty Liver Disease. *J Gastroenterol*.

Javitt NB (2008) Oxysterols: Novel Biologic Roles for the 21st Century. *Steroids* **73**:149-157.

Javitt NB, Lee Y C, Shimizu C, Fuda H and Strott C A (2001) Cholesterol and Hydroxycholesterol Sulfotransferases: Identification, Distinction From Dehydroepiandrosterone Sulfotransferase, and Differential Tissue Expression. *Endocrinology* **142**:2978-2984.

Jiang XC, Qin S, Qiao C, Kawano K, Lin M, Skold A, Xiao X and Tall A R (2001) Apolipoprotein B Secretion and Atherosclerosis Are Decreased in Mice With Phospholipid-Transfer Protein Deficiency. *Nat Med* **7**:847-852.

Korach-Andre M, Parini P, Larsson L, Arner A, Steffensen K R and Gustafsson J A (2010) Separate and Overlapping Metabolic Functions of LXRalpha and LXRbeta in C57Bl/6 Female Mice. *Am J Physiol Endocrinol Metab* **298**:E167-E178.

Li J, Viswanadha S and Loor J J (2012) Hepatic Metabolic, Inflammatory, and Stress-Related Gene Expression in Growing Mice Consuming a Low Dose of Trans-10, Cis-12-Conjugated Linoleic Acid. *J Lipids* **2012**:571281.

Li T, Owsley E, Matozel M, Hsu P, Novak C M and Chiang J Y (2010) Transgenic Expression of Cholesterol 7alpha-Hydroxylase in the Liver Prevents High-Fat Diet-Induced Obesity and Insulin Resistance in Mice. *Hepatology* **52**:678-690.

Li X, Hylemon P, Pandak W M and Ren S (2006) Enzyme Activity Assay for Cholesterol 27-Hydroxylase in Mitochondria. *J Lipid Res* **47**:1507-1512.

Li X, Pandak W M, Erickson S K, Ma Y, Yin L, Hylemon P and Ren S (2007) Biosynthesis of the Regulatory Oxysterol, 5-Cholesten-3beta,25-Diol 3-Sulfate, in Hepatocytes. *J Lipid Res* **48**:2587-2596.

Ma Y, Xu L, Rodriguez-Agudo D, Li X, Heuman D M, Hylemon P B, Pandak W M and Ren S (2008) 25-Hydroxycholesterol-3-Sulfate Regulates Macrophage Lipid Metabolism Via the LXR/SREBP-1 Signaling Pathway. *Am J Physiol Endocrinol Metab* **295**:E1369-E1379.

Malhi H, Bronk S F, Werneburg N W and Gores G J (2006) Free Fatty Acids Induce JNK-Dependent Hepatocyte Lipoapoptosis. *J Biol Chem* **281**:12093-12101.

Malhi H and Gores G J (2008) Molecular Mechanisms of Lipotoxicity in Nonalcoholic Fatty Liver Disease. *Semin Liver Dis* **28**:360-369.

Manco M, Marcellini M, Giannone G and Nobili V (2007) Correlation of Serum TNF-Alpha Levels and Histologic Liver Injury Scores in Pediatric Nonalcoholic Fatty Liver Disease. *Am J Clin Pathol* **127**:954-960.

Mazza A, Fruci B, Garinis G A, Giuliano S, Malaguarnera R and Belfiore A (2012) The Role of Metformin in the Management of NAFLD. *Exp Diabetes Res* **2012**:716404.

Neuschwander-Tetri BA (2010) Hepatic Lipotoxicity and the Pathogenesis of Nonalcoholic Steatohepatitis: the Central Role of Nontriglyceride Fatty Acid Metabolites. *Hepatology* **52**:774-788.

Ogawa S, Kakiyama G, Muto A, Hosoda A, Mitamura K, Ikegawa S, Hofmann A F and Iida T (2009) A Facile Synthesis of C-24 and C-25 Oxysterols by in Situ Generated Ethyl(Trifluoromethyl)Dioxirane. *Steroids* **74**:81-87.

Okazaki H, Goldstein J L, Brown M S and Liang G (2010) LXR-SREBP-1c-Phospholipid Transfer Protein Axis Controls Very Low Density Lipoprotein (VLDL) Particle Size. *J Biol Chem* **285**:6801-6810.

Polyzos SA, Kountouras J and Mantzoros C S (2012) Sulfated Oxysterols As Candidates for the Treatment of Nonalcoholic Fatty Liver Disease. *Metabolism* **61**:755-758.

Reddy JK and Rao M S (2006) Lipid Metabolism and Liver Inflammation. II. Fatty Liver Disease and Fatty Acid Oxidation. *Am J Physiol Gastrointest Liver Physiol* **290**:G852-G858.

Ren S, Hylemon P, Marques D, Hall E, Redford K, Gil G and Pandak W M (2004) Effect of Increasing the Expression of Cholesterol Transporters (StAR, MLN64, and SCP-2) on Bile Acid Synthesis. *J Lipid Res* **45**:2123-2131.

Ren S, Hylemon P, Zhang Z P, Rodriguez-Agudo D, Marques D, Li X, Zhou H, Gil G and Pandak W M (2006) Identification of a Novel Sulfonated Oxysterol, 5-Cholesten-3beta,25-Diol 3-Sulfonate, in Hepatocyte Nuclei and Mitochondria. *J Lipid Res* **47**:1081-1090.

Ren S, Li X, Rodriguez-Agudo D, Gil G, Hylemon P and Pandak W M (2007) Sulfated Oxysterol, 25HC3S, Is a Potent Regulator of Lipid Metabolism in Human Hepatocytes. *Biochem Biophys Res Commun* **360**:802-808.

Samuel VT and Shulman G I (2012) Mechanisms for Insulin Resistance: Common Threads and Missing Links. *Cell* **148**:852-871.

Snyder VL, Turner M, Li P K, El Sharkawy A, Dunphy G and Ely D L (2000) Tissue Steroid Sulfatase Levels, Testosterone and Blood Pressure. *J Steroid Biochem Mol Biol* **73**:251-256.

Tilg H and Moschen A R (2010) Evolution of Inflammation in Nonalcoholic Fatty Liver Disease: the Multiple Parallel Hits Hypothesis. *Hepatology* **52**:1836-1846.

Tiniakos DG, Vos M B and Brunt E M (2010) Nonalcoholic Fatty Liver Disease: Pathology and Pathogenesis. *Annu Rev Pathol* **5**:145-171.

Torocsik D, Szanto A and Nagy L (2009) Oxysterol Signaling Links Cholesterol Metabolism and Inflammation Via the Liver X Receptor in Macrophages. *Mol Aspects Med* **30**:134-152.

Vallim T and Salter A M (2010) Regulation of Hepatic Gene Expression by Saturated Fatty Acids. *Prostaglandins Leukot Essent Fatty Acids* **82**:211-218.

van Reyk DM, Brown A J, Hult'en L M, Dean R T and Jessup W (2006) Oxysterols in Biological Systems: Sources, Metabolism and Pathophysiological Relevance. *Redox Rep* **11**:255-262.

Xu L, Bai Q, Rodriguez-Agudo D, Hylemon P B, Heuman D M, Pandak W M and Ren S (2010) Regulation of Hepatocyte Lipid Metabolism and Inflammatory Response by 25-Hydroxycholesterol and 25-Hydroxycholesterol-3-Sulfate. *Lipids* **45**:821-832.

Xu L, Shen S, Ma Y, Kim J K, Rodriguez-Agudo D, Heuman D M, Hylemon P B, Pandak W M and Ren S (2012) 25-Hydroxycholesterol-3-Sulfate Attenuates Inflammatory Response Via PPARgamma Signaling in Human THP-1 Macrophages. *Am J Physiol Endocrinol Metab* **302**:E788-E799.

Zhang Z, Li D, Blanchard D E, Lear S R, Erickson S K and Spencer T A (2001) Key Regulatory Oxysterols in Liver: Analysis As Delta4-3-Ketone Derivatives by HPLC and Response to Physiological Perturbations. *J Lipid Res* **42**:649-658.

Footnotes:

This work was supported by National Institutes of Health [5R01HL078898] and VA Merit Review [821 (Program Number) 103 (Cost Center)] from Veterans Affairs Administration.

Address reprint requests to: Dr. Shunlin Ren, McGuire Veterans Affairs Medical Center, Research 151, 1201 Broad Rock Blvd, Richmond, VA 23249. E-mail: sren@vcu.edu

Molecular Pharmacology Fast Forward. Published on December 20, 2012 as DOI: 10.1124/mol.112.081505
This article has not been copyedited and formatted. The final version may differ from this version.

Legends

Figure 1. Effects of 25HC3S on the serum lipid profiles in HFD-fed mice. Eight-week-old C57BL/6J female mice were fed a high fat diet (HFD) or chow diet (Chow) for 10 weeks, treated with either 25HC3S or vehicle twice and fasted over night. Plasma triglyceride (Panel **A**), total cholesterol (Panel **B**) and high-density lipoprotein cholesterol (Panel **C**) were determined. All the values are expressed as mean ± SEM. Statistical significance ** $p < 0.01$ versus chow diet-fed vehicle-treated mice liver; † $p < 0.05$, †† $p < 0.01$ versus HFD-fed vehicle-treated mice liver, n=15-17. Serum lipoprotein were separated by HPLC with a Superose 6 column (Panel **D**), and each fraction was collected for the measurement of concentration of triglyceride (Panel **E**) and cholesterol (Panel **F**). The data represent one of three separate experiments. TG, triglyceride; CHOL, cholesterol; HDL-C, high-density lipoprotein cholesterol.

Figure 2. HPLC Analysis of 25HC3S and 25HC levels in the treated mice liver tissues. Animals were treated as described in Figure 1. Total neutral lipids were extracted with chloroform/methanol mixture and analyzed by HPLC. 24-hydroxycholesterol (24HC), 25-hydroxycholesterol (25HC), 27-hydroxycholesterol (27HC) and 7α-hydroxycholesterol (7α-HC) were used as standard controls; and Testosterone in chloroform phase was used as an internal control. Oxysterols in chloroform phase from vehicle- or 25HC3S-treated mouse liver were determined (**Left panel**). Chemical synthesis of 25HC3S was used as standard control in water/methanol phase. 25HC3S in water/methanol phase from vehicle- and 25HC3S-treated mice liver were determined (**Right panel**). The data represent one of three separate experiments.

Figure 3. The effects of 25HC3S on protein expressions in lipid metabolism in liver tissues.

Molecular Pharmacology Fast Forward. Published on December 20, 2012 as DOI: 10.1124/mol.112.081505
This article has not been copyedited and formatted. The final version may differ from this version.

Animals were treated as described in Figure 1. Specific protein levels in cytoplasmic and nuclear extracts were determined by Western blot analysis. Cytoplasmic ACC1 and FAS protein levels were shown in Panel **A**, normalized by β-actin; and nuclear SREBP1 and SREBP2 (**B**), normalized by Lamin B1. All the values are expressed as mean ± SEM. Statistical significance # $p < 0.05$ versus chow diet-fed vehicle-treated mice liver; * $p < 0.05$ versus HFD-fed vehicle-treated mice liver; (n=6-8).

Figure 4. The effects of long term-treatment with 25HC3S on mouse body mass and food intake. C57BL/6J female mice were fed with HFD, separated to two groups, and treated with either 25HC3S or vehicle once every three days for 6 weeks. During these 6 weeks, the total food intake (**A**) and the body weight were monitored (**B**). After 5 hours fasting, the liver weight was determined (**C**), the plasma alkaline phosphatase (ALK) (**D**), alanine aminotransferase (ALT) (**E**) and aspartate aminotransferase (AST) (**F**) were determined. All the values are expressed as mean ± SEM (n=10). Statistical significance * $p < 0.05$ and ** $p < 0.01$ versus HFD-fed vehicle-treated mouse liver.

Figure 5. A long-term treatment with 25HC3S decrases lipid accumulation in the liver tissue in mouse NAFLD models. Animals were treated as described in Figure 4. Hepatic triglyceride (**A**); free fatty acid (**B**); total cholesterol (**C**); free cholesterol (**D**); and cholesterol ester (**E**). Each individual level was normalized by liver weight. All the values are expressed as mean ± SD. Statistical significance # $p < 0.001$ versus chow-fed vehicle-treated mice. * $p < 0.05$ and ** $p < 0.01$ versus HFD-fed vehicle-treated mice liver. In morphology study, liver sections from chow diet fed (**chow**), high fat diet fed (**HFD**) and high fat diet fed with 25HC3S treated (**HFD-25HC3S**) mice were stained by H&E staining. Arrows indicate unstained lipid inclusions.

Molecular Pharmacology Fast Forward. Published on December 20, 2012 as DOI: 10.1124/mol.112.081505
This article has not been copyedited and formatted. The final version may differ from this version.

Figure 6. A long-term treatment with 25HC3S improved insulin sensitivity and glucose homeostasis in HFD-fed mice. Animals were treated as described in Figure 4. GTT (**A**) and ITT (**B**) were performed. All the values are expressed as mean ± SEM (n=9-10). * $p < 0.05$ and ** $p < 0.01$ versus HFD-fed vehicle-treated mice. Abbreviations: GTT, glucose tolerance test; ITT, insulin tolerance test; HFD, high fat diet; Cont, control vehicle.

Molecular Pharmacology Fast Forward. Published on December 20, 2012 as DOI: 10.1124/mol.112.081505
This article has not been copyedited and formatted. The final version may differ from this version.

Table 1. Relative Hepatic mRNA Expression in the Mice Fed a HFD with or without 25HC3S

Gene Name	Gene description	HFD			HFD + 25HC3S		
Fatty acid biosynthesis							
SREBP-1c	Sterol regulatory element-binding protein-1c	1	±	0.09	**0.54**	±	**0.13 ****
ACC1	Acetyl-CoA carboxylase 1	1	±	0.20	**0.43**	±	**0.12 ****
FAS	Fatty acid synthase	1	±	0.37	**0.51**	±	**0.37 ***
LXRα	Liver X receptor α	1	±	0.20	0.90	±	0.42
FABP1	Fatty acid binding protein 1	1	±	0.23	1.15	±	0.46
FATP1	Fatty acid transport protein 1	1	±	0.38	1.03	±	0.28
Fatty acid oxidation							
PPARα	Peroxisome proliferator-activated receptor α	1	±	0.37	0.95	±	0.36
CPT1	Carnitine palmitoyltransferase 1	1	±	0.24	1.07	±	0.19
ACOX1	Acyl-CoA oxidase 1	1	±	0.23	0.79	±	0.16
MCAD	Medium chain acyl-CoA dehydrogenase	1	±	0.19	1.30	±	0.29
SCAD	Short chain acyl-CoA dehydrogenase	1	±	0.21	0.95	±	0.28
Triglyceride metabolism							
GPAM	Glycerol-3-phosphate acyltransferase	1	±	0.22	1.06	±	0.07
MTTP	Microsomal triglyceride transfer protein	1	±	0.30	1.11	±	0.17
PLTP	Phospholipid transfer protein	1	±	0.17	0.96	±	0.54
Cholesterol metabolism							
SREBP-2	Sterol regulatory element-binding protein-2	1	±	0.30	1.07	±	0.11
HMGR	Hydroxy-methylglutaryl-coenzyme A reductase	1	±	0.41	0.94	±	0.18
ABCA1	ATP-binding cassette, sub-family A1	1	±	0.16	**0.70**	±	**0.12 ****
ABCG1	ATP-binding cassette, sub-family G1	1	±	0.44	0.99	±	0.65
ABCG5	ATP-binding cassette, sub-family G5	1	±	0.15	0.99	±	0.30
CYP7α	Cholesterol 7α-hydroxylase	1	±	0.27	**0.55**	±	**0.17 ***
CYP27α	Mitochondrial cholesterol 27a-hydroxylase	1	±	0.12	1.06	±	0.22
Lipid uptake							
LDLR	Low density lipoprotein receptor	1	±	0.43	0.91	±	0.07
CD36	Thrombospondin receptor	1	±	0.27	0.93	±	0.36
SRB1	Scavenger receptor class B, member 1	1	±	0.12	1.25	±	0.22
Inflammatory response							
PPARγ	Peroxisome proliferator-activated receptor gamma	1	±	0.23	**1.63**	±	**0.41 ***
IκBα	Nuclear factor of kappa light polypeptide gene enhancer in B-cells inhibitor α	1	±	0.20	1.04	±	0.14
TNFα	Tumor necrosis factor α	1	±	0.21	**0.65**	±	**0.28 ***
NFκB (Rela)	V-rel reticuloendotheliosis viral oncogene homolog A	1	±	0.22	0.83	±	0.19
IL1α	Interleukin 1α	1	±	0.29	0.92	±	0.23
IL1β	Interleukin 1β	1	±	0.78	1.11	±	0.64
Glucose metabolism							
G6Pase	Glucose-6-phosphatase	1	±	0.23	1.23	±	0.70
PCK1	Phosphoenolpyruvate carboxykinase 1	1	±	0.20	1.07	±	0.26
GCK	Glucokinase	1	±	0.21	1.21	±	0.75
Pklr	Pyruvate kinase, liver and RBC	1	±	0.22	**0.56**	±	**0.16 ****

Animals were treated as described in Figure 1. All values are expressed as the mean ± SD; n = 5-6. *$p < 0.05$, **$p < 0.01$ compared with HFD mice.

Molecular Pharmacology Fast Forward. Published on December 20, 2012 as DOI: 10.1124/mol.112.081505
This article has not been copyedited and formatted. The final version may differ from this version.

Table 2. Relative Hepatic mRNA Expression in the Mice Fed a HFD with or without 25HC3S

Gene Name	Gene description	HFD			HFD + 25HC3S		
Fatty acid biosynthesis							
SREBP-1c	Sterol regulatory element-binding protein-1c	1	±	0.12	**0.77**	±	**0.06 ***
ACC1	Acetyl-CoA carboxylase 1	1	±	0.33	**0.59**	±	**0.05 ***
FAS	Fatty acid synthase	1	±	0.47	**0.73**	±	**0.07 ***
LXRα	Liver X receptor α	1	±	0.27	1.07	±	0.45
FABP1	Fatty acid binding protein 1	1	±	0.36	0.98	±	0.41
FATP1	Fatty acid transport protein 1	1	±	0.53	0.69	±	0.25
Fatty acid oxidation							
PPARα	Peroxisome proliferator-activated receptor α	1	±	0.16	0.81	±	0.18
CPT1	Carnitine palmitoyltransferase 1	1	±	0.16	**0.79**	±	**0.11 ***
ACOX1	Acyl-CoA oxidase 1	1	±	0.21	0.95	±	0.14
MCAD	Medium chain acyl-CoA dehydrogenase	1	±	0.15	**0.80**	±	**0.15 ***
SCAD	Short chain acyl-CoA dehydrogenase	1	±	0.12	0.95	±	0.14
Triglyceride metabolism							
GPAM	Glycerol-3-phosphate acyltransferase	1	±	0.21	**0.79**	±	**0.08 ***
MTTP	Microsomal triglyceride transfer protein	1	±	0.22	**0.77**	±	**0.07 ***
PLTP	Phospholipid transfer protein	1	±	0.43	**0.61**	±	**0.07 ***
Cholesterol metabolism							
SREBP-2	Sterol regulatory element-binding protein-2	1	±	0.26	1.07	±	0.31
HMGR	Hydroxy-methylglutaryl-coenzyme A reductase	1	±	0.09	1.19	±	0.22
ABCA1	ATP-binding cassette, sub-family A	1	±	0.11	**0.79**	±	**0.10 ***
ABCG1	ATP-binding cassette, sub-family G	1	±	0.24	**0.66**	±	**0.13 ***
CYP7α	Cholesterol 7α-hydroxylase	1	±	0.59	0.68	±	0.34
CYP27α	Mitochondrial cholesterol 27a-hydroxylase	1	±	0.17	0.91	±	0.15
Lipid uptake							
LDLR	Low density lipoprotein receptor	1	±	0.39	0.80	±	0.21
CD36	Thrombospondin receptor	1	±	0.24	**0.52**	±	**0.04 ****
SRB1	Scavenger receptor class B, member 1	1	±	0.17	**0.79**	±	**0.06 ***
Inflammatory response							
PPARγ	Peroxisome proliferator-activated receptor gamma	1	±	0.23	0.78	±	0.21
IκBα	Nuclear factor of kappa light polypeptide gene enhancer in B-cells inhibitor α	1	±	0.31	1.11	±	0.66
NFκB (Rela)	V-rel reticuloendotheliosis viral oncogene homolog A	1	±	0.33	1.00	±	0.48
TNFα	Tumor necrosis factor α	1	±	0.20	**0.53**	±	**0.18 ***
IL1α	Interleukin 1α	1	±	0.30	**0.52**	±	**0.07 ***
IL1β	Interleukin 1β	1	±	0.49	**0.50**	±	**0.14 ***
Glucose metabolism							
G6Pase	Glucose-6-phosphatase	1	±	0.31	1.05	±	0.44
PCK1	Phosphoenolpyruvate carboxykinase 1	1	±	0.20	1.30	±	0.99
GCK	Glucokinase	1	±	0.30	1.19	±	0.67
Pklr	Pyruvate kinase, liver and RBC	1	±	0.17	0.97	±	0.17

Animals were treated as described in Figure 4. All values are expressed as the mean ± SD; n = 5-6. *$p < 0.05$, **$p < 0.01$ compared with HFD mice. Abbreviations: HFD, high fat diet.

Figure 1

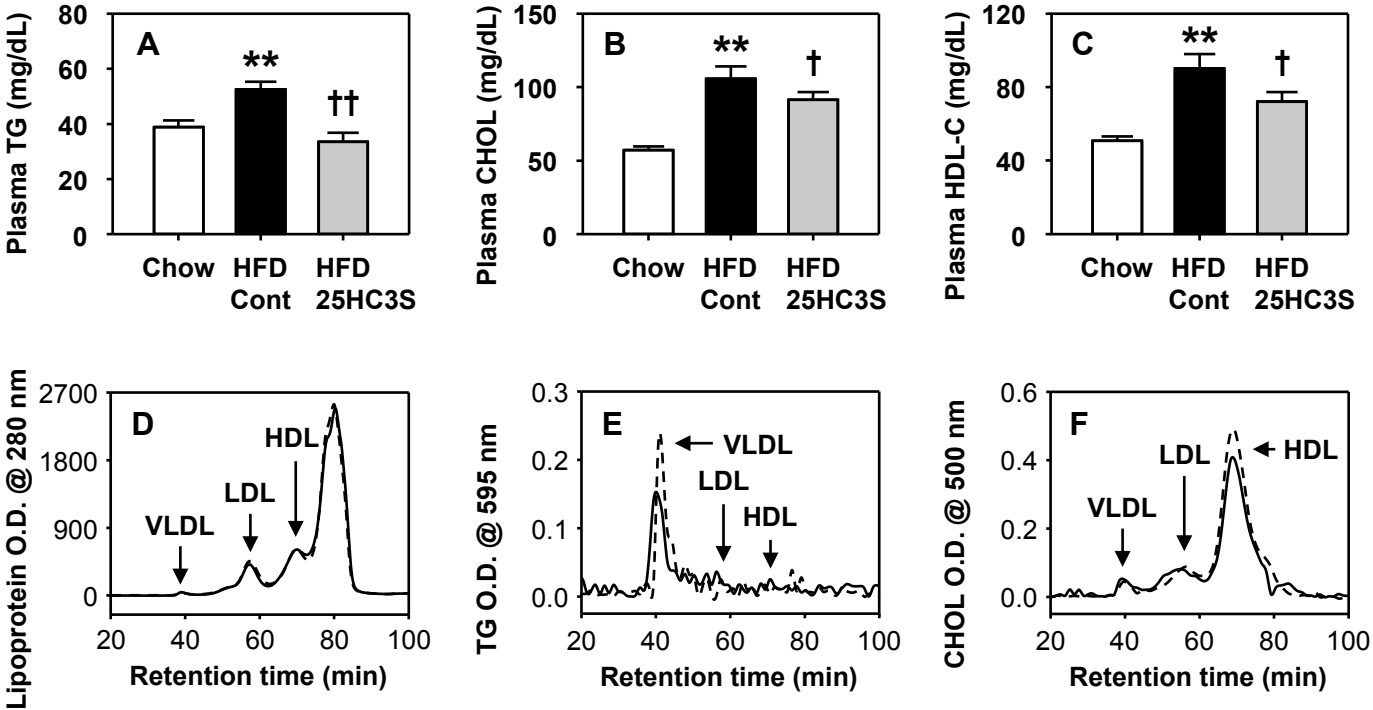
A
Plasma TG (mg/dL)
80
60
40
20
0
**
††
Chow
HFD Cont
HFD 25HC3S
B
Plasma CHOL (mg/dL)
150
100
50
0
**
†
Chow
HFD Cont
HFD 25HC3S
C
Plasma HDL-C (mg/dL)
120
80
40
0
**
†
Chow
HFD Cont
HFD 25HC3S
D
Lipoprotein O.D. @ 280 nm
2700
1800
900
0
VLDL
LDL
HDL
20
40
60
80
100
Retention time (min)
E
TG O.D. @ 595 nm
0.3
0.2
0.1
0.0
VLDL
LDL
HDL
20
40
60
80
100
Retention time (min)
F
CHOL O.D. @ 500 nm
0.6
0.4
0.2
0.0
VLDL
LDL
HDL
20
40
60
80
100
Retention time (min)

Figure 2

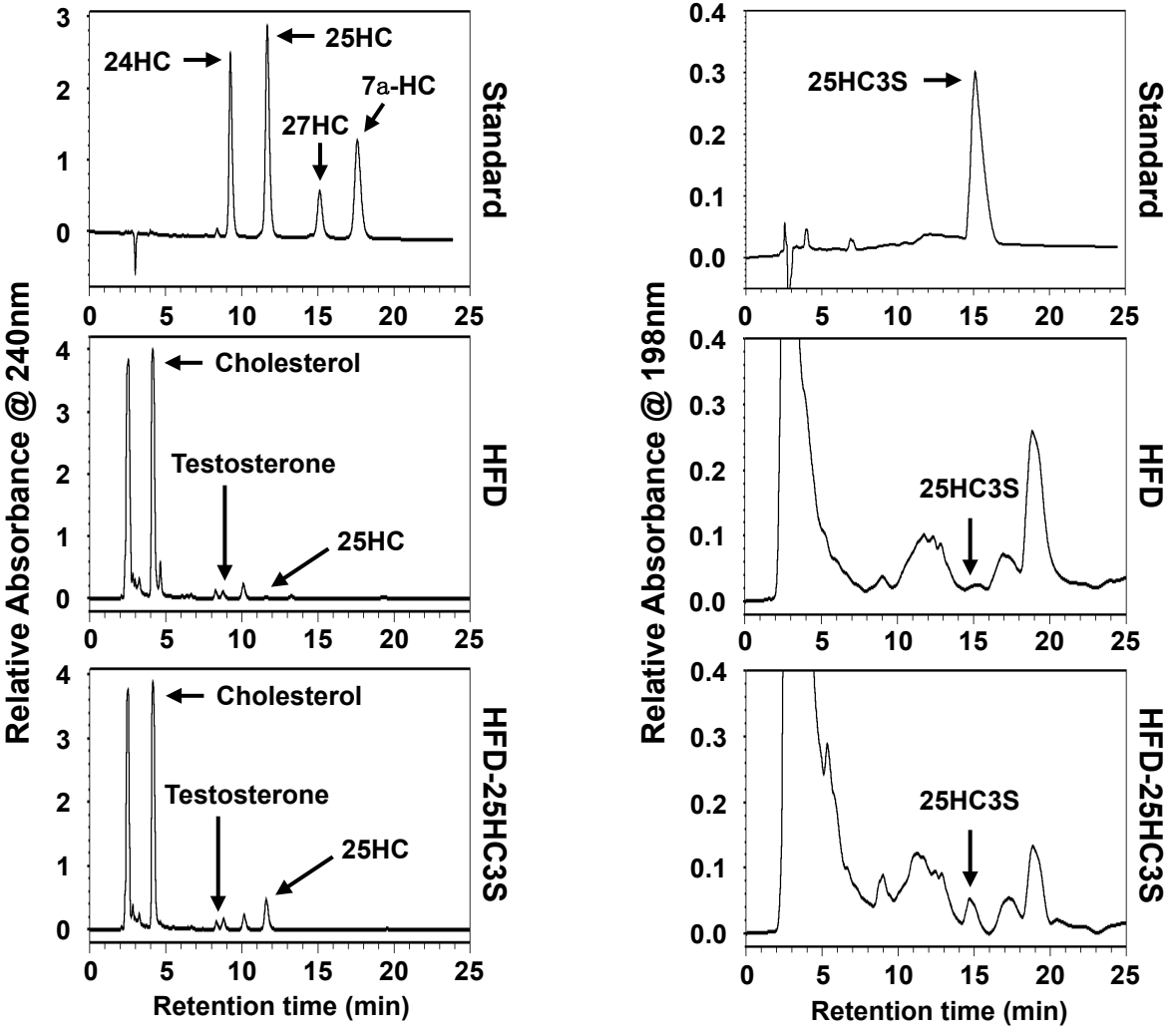
24HC
25HC
7a-HC
27HC
Standard
Cholesterol
Testosterone
25HC
HFD
Cholesterol
Testosterone
25HC
HFD-25HC3S
Relative Absorbance @ 240nm
Retention time (min)
25HC3S
Standard
25HC3S
HFD
25HC3S
HFD-25HC3S
Relative Absorbance @ 198nm
Retention time (min)

Figure 3

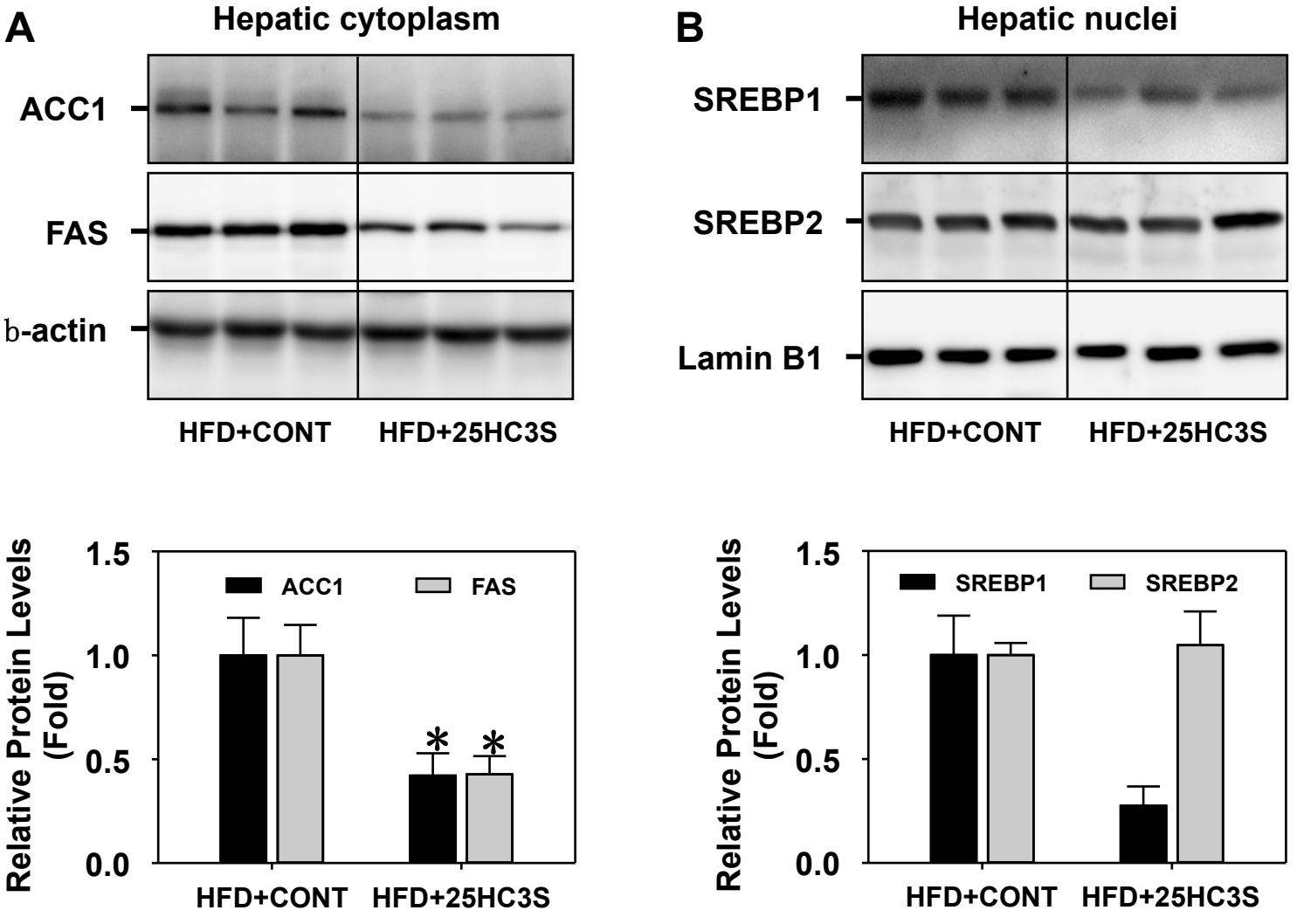
A
Hepatic cytoplasm
ACC1
FAS
b-actin
HFD+CONT
HFD+25HC3S
B
Hepatic nuclei
SREBP1
SREBP2
Lamin B1
HFD+CONT
HFD+25HC3S
Relative Protein Levels (Fold)
1.5
1.0
0.5
0.0
ACC1
FAS
*
*
HFD+CONT
HFD+25HC3S
Relative Protein Levels (Fold)
1.5
1.0
0.5
0.0
SREBP1
SREBP2
HFD+CONT
HFD+25HC3S

Figure 4

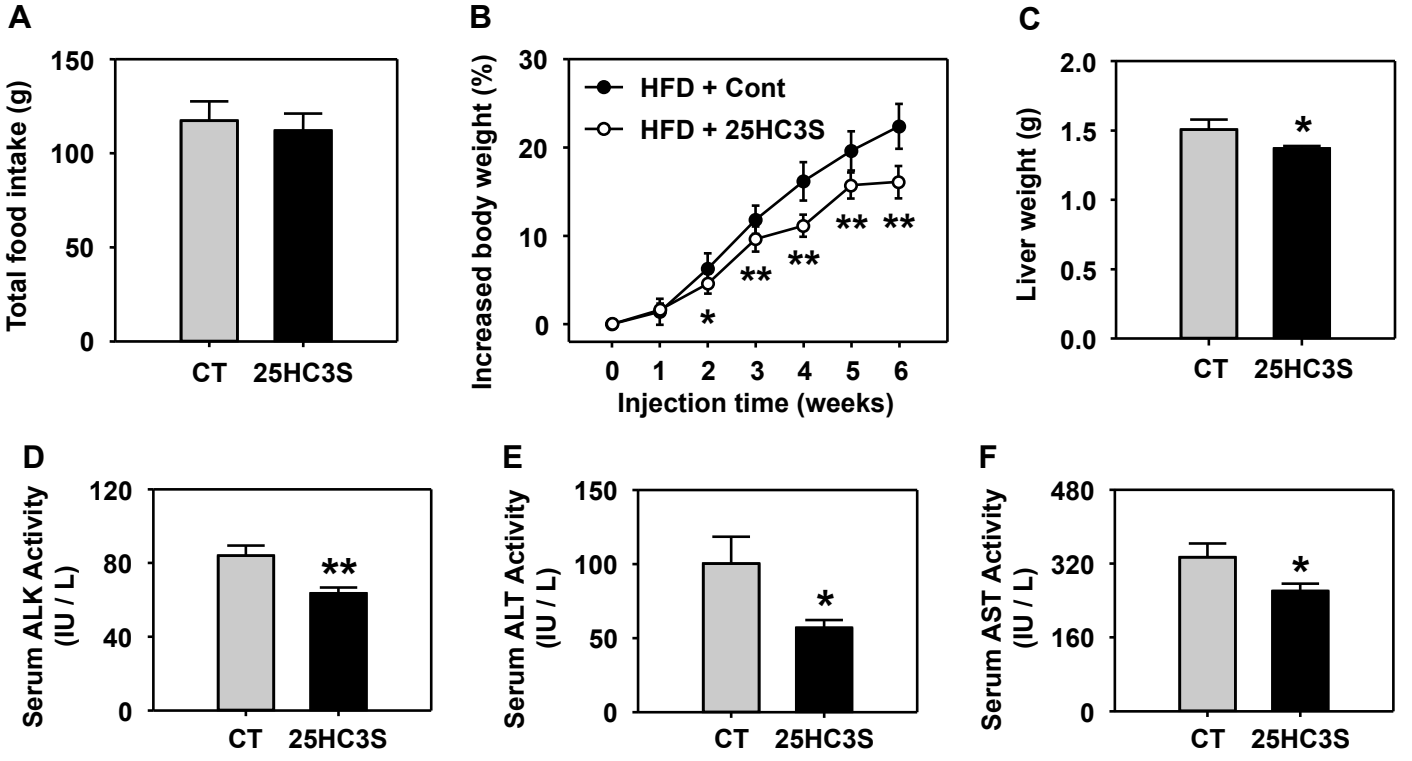
A
Total food intake (g)
150
100
50
0
CT
25HC3S
B
Increased body weight (%)
30
20
10
0
HFD + Cont
HFD + 25HC3S
*
**
**
**
**
0 1 2 3 4 5 6
Injection time (weeks)
C
Liver weight (g)
2.0
1.5
1.0
0.5
0.0
*
CT
25HC3S
D
Serum ALK Activity (IU / L)
120
80
40
0
**
CT
25HC3S
E
Serum ALT Activity (IU / L)
150
100
50
0
*
CT
25HC3S
F
Serum AST Activity (IU / L)
480
320
160
0
*
CT
25HC3S

Figure 5

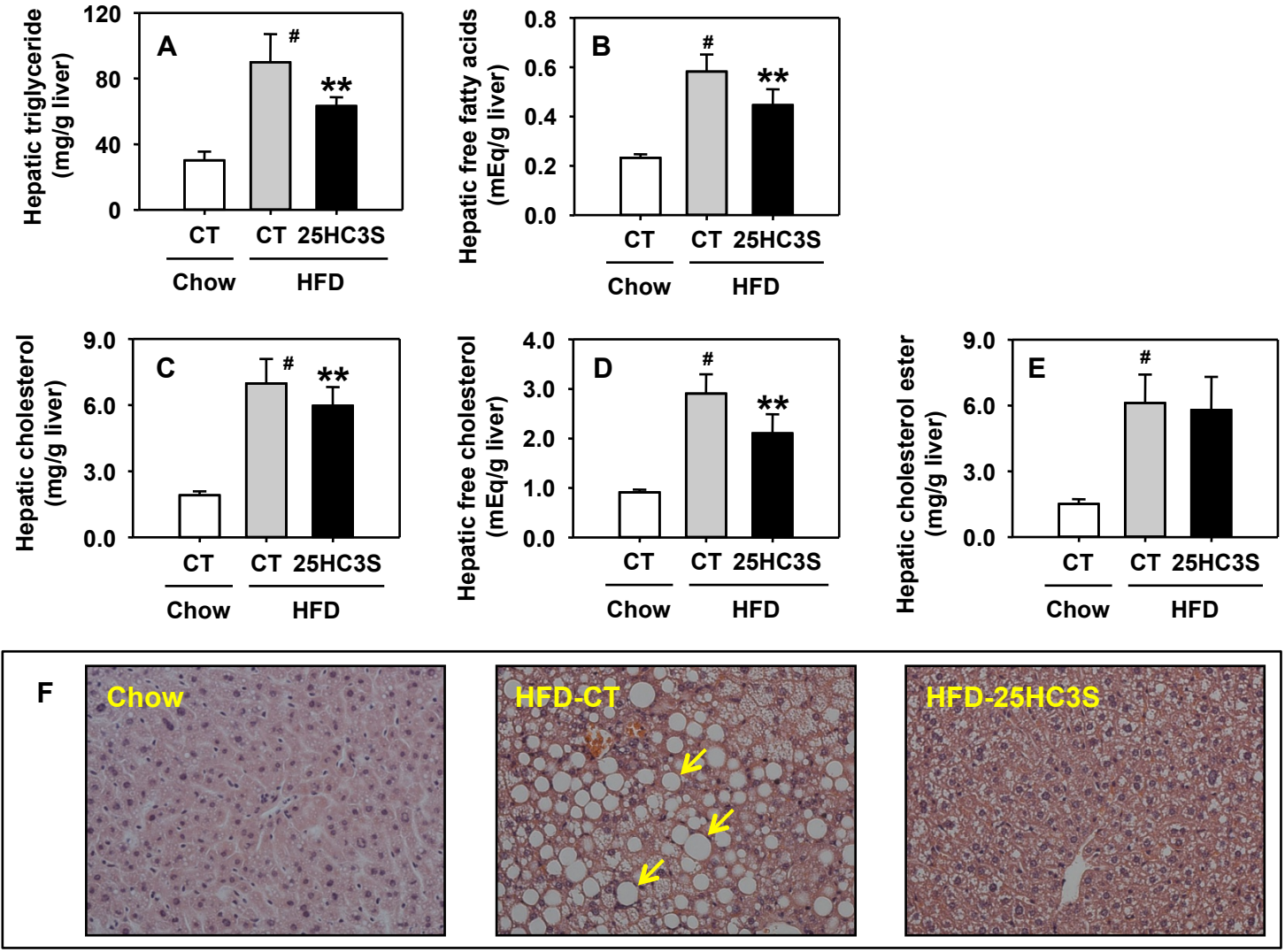
A
Hepatic triglyceride (mg/g liver)
120
80
40
0
#
**
CT
CT 25HC3S
Chow
HFD
B
Hepatic free fatty acids (mEq/g liver)
0.8
0.6
0.4
0.2
0.0
#
**
CT
CT 25HC3S
Chow
HFD
C
Hepatic cholesterol (mg/g liver)
9.0
6.0
3.0
0.0
#
**
CT
CT 25HC3S
Chow
HFD
D
Hepatic free cholesterol (mEq/g liver)
4.0
3.0
2.0
1.0
0.0
#
**
CT
CT 25HC3S
Chow
HFD
E
Hepatic cholesterol ester (mg/g liver)
9.0
6.0
3.0
0.0
#
CT
CT 25HC3S
Chow
HFD
F
Chow
HFD-CT
HFD-25HC3S

Figure 6

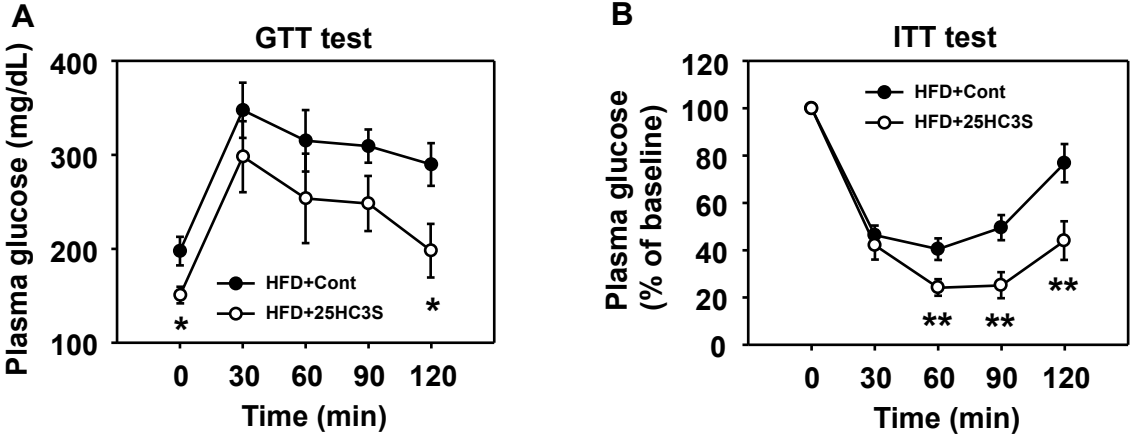
A
GTT test
Plasma glucose (mg/dL)
400
300
200
100
HFD+Cont
HFD+25HC3S
*
*
0
30
60
90
120
Time (min)
B
ITT test
Plasma glucose (% of baseline)
120
100
80
60
40
20
0
HFD+Cont
HFD+25HC3S
**
**
**
0
30
60
90
120
Time (min)

Molecular Pharmacology

Supplementary Information

5-Cholesten-3β,25-diol 3-sulfate Decreases Lipid Accumulation in Diet-induced Nonalcoholic Fatty Liver Disease Mouse Model

Leyuan Xu, Jin Koung Kim, Qianming Bai, Xin Zhang, Genta Kakiyama, Hae-ki Min, Arun J. Sanyal, William M. Pandak, and Shunlin Ren

Department of Internal Medicine, Virginia Commonwealth University and McGuire Veterans Affairs Medical Center, Richmond, VA, USA

Supplementary Figure 1. Mass spectral analysis of 25HC3S.

Characterization of the chemically synthesized and purified 5-cholesten-3β,25-diol 3-sulfonate was analyzed by negative ion-triple quadrapole mass spectrometer (Peking University, China), which shows the same molecular mass ion, *m/z* 481 as the "authentic" nuclear oxysterol and the purified product was not contaminated by the starting material, 25-hydroxycholesterol, *m/z* 401.

Supplementary Figure 2. Proton nuclear magnetic resonance spectroscopy of 25HC3S.

1H NMR analysis shows that the proton resonance at C3 with multiple small (1.5 Hz) splits near 3.65 ppm in the spectrum of 25-hydroxycholesterol (starting material) is shifted to 4.20 ppm in the product spectrum, which confirms that a HSO3− group is added at the C3 position of 25-hydroxycholesterol. The results indicate that the synthesized molecule is 5-cholesten-3β,25-diol 3-sulfonate (25HC3S).

Supplementary Table. 1. Primer sets for real time RT-PCR analysis of gene expression

Name	GenBank No.	Forward Sequence	Reverse Sequence
SREBP-1c	NM_011480	AGCAGCCCCTAGAACAAACAC	CAGCAGTGAGTCTGCCTTGAT
ACC1	NM_133360	ATGGGCGGAATGGTCTCTTTC	TGGGGACCTTGTCTTCATCAT
FAS	NM_007988	AGAGATCCCGAGACGCTTCT	GCCTGGTAGGCATTCTGTAGT
LXRα	NM_013839	GAGCCGACAGAGCTTCGTC	GCGTGCTCCCTTGATGACA
CPT1	NM_013495	CTCCGCCTGAGCCATGAAG	CACCAGTGATGATGCCATTCT
PPARα	NM_011144	AGAGCCCCATCTGTCCTCTC	ACTGGTAGTCTGCAAAACCAAA
ACOX1	NM_015729	TCCAGACTTCCAACATGAGGA	CTGGGCGTAGGTGCCAATTA
MCAD	NM_007382	AGGGTTTAGTTTTGAGTTGACGG	CCCCGCTTTTGTCATATTCCG
SCAD	NM_007383	ACAGTGGATCACCCCTTTCAC	ACCCATGAGTCACCCTCTTCC
PPARγ	NM_008904	TATGGAAGTGACATAGAGTGTGCT	CCACTTCAATCCACCCAGAAAG
FABP1	NM_017399	CTGACACCCCCTTGATGTCC	ATGAACTTCTCCGGCAAGTAC
FATP1	NM_011977	CGCTTTCTGCGTATCGTCTG	GATGCACGGGATCGTGTCT
GPAM	NM_008149	ACAGTTGGCACAATAGACGTTT	CCTTCCATTTCAGTGTTGCAGA
MTTP	NM_008642	CTCTTGGCAGTGCTTTTTCTCT	GAGCTTGTATAGCCGCTCATT
PLTP	NM_011125	CGCAAAGGGCCACTTTTACTA	GCCCCCATCATATAAGAACCAG
SREBP-2	NM_033218	TGAAGGACTTAGTCATGGGGAC	CGCAGCTTGTGATTGACCT
HMGR	NM_008255	AGCTTGCCCGAATTGTATGTG	TCTGTTGTGAACCATGTGACTTC
ABCA1	NM_013454	AAAACCGCAGACATCCTTCAG	CATACCGAAACTCGTTCACCC
ABCG1	NM_009593	GCTCCATCGTCTGTACCATCC	TGTTCTGATCCCCGTACTCCC
ABCG5	NM_031884	ATTATGTGCATCTTAGGCAGCTC	CGTAGGAGAAGCAGTCTTGGAA
CYP7α	NM_007824	AACGGGTTGATTCCATACCTGG	GTGGACATATTTCCCCATCAGTT
CYP27α	NM_024264	GACAACCTCCTTTGGGACTTAC	GTGGTCTCTTATTGGGTACTTGC
LDLR	NM_010700	AGTGGCCCCGAATCATTGAC	CTAACTAAACACCAGACAGAGGC
SRB1	NM_016741	TTTGGAGTGGTAGTAAAAAGGGC	TGACATCAGGGACTCAGAGTAG
CD36	NM_007643	ATGGGCTGTGATCGGAACTG	GTCTTCCCAATAAGCATGTCTCC
G6Pase	NM_008061	TCGGAGACTGGTTCAACCTC	AGGTGACAGGGAACTGCTTTAT
PCK1	NM_011044	CTGCATAACGGTCTGGACTTC	CAGCAACTGCCCGTACTCC
GCK	NM_010292	AGGAGGCCAGTGTAAAGATGT	CTCCCAGGTCTAAGGAGAGAAG
Pklr	NM_013631	TCAAGGCAGGGATGAACATTG	CACGGGTCTGTAGCTGAGTG
IL1α	NM_010554	CTGATGAAGCTCGTCAGGCAG	TGGTGCTGAGATAGTGTTTGTC
IL1β	NM_008361	GCAACTGTTCCTGAACTCAACT	ATCTTTTGGGGTCCGTCAACT
NFκB (Rela)	NM_009045	GCGCGGGGACTATGACTTG	GCCCGGTTATCAAAAATCGGAT
TNFα	NM_013693	CCCTCACACTCAGATCATCTTCT	GCTACGACGTGGGCTACAG
IκBα	NM_010907	TGAAGGACGAGGAGTACGAGC	TTCGTGGATGATTGCCAAGTG
GAPDH	NM_008084	CATGTTCCAGTATGACTCCACTC	GGCCTCACCCCATTTGATGT
β-actin	NM_007393	GGCTGTATTCCCCTCCATCG	CCAGTTGGTAACAATGCCATGT

Supplementary Figure 1

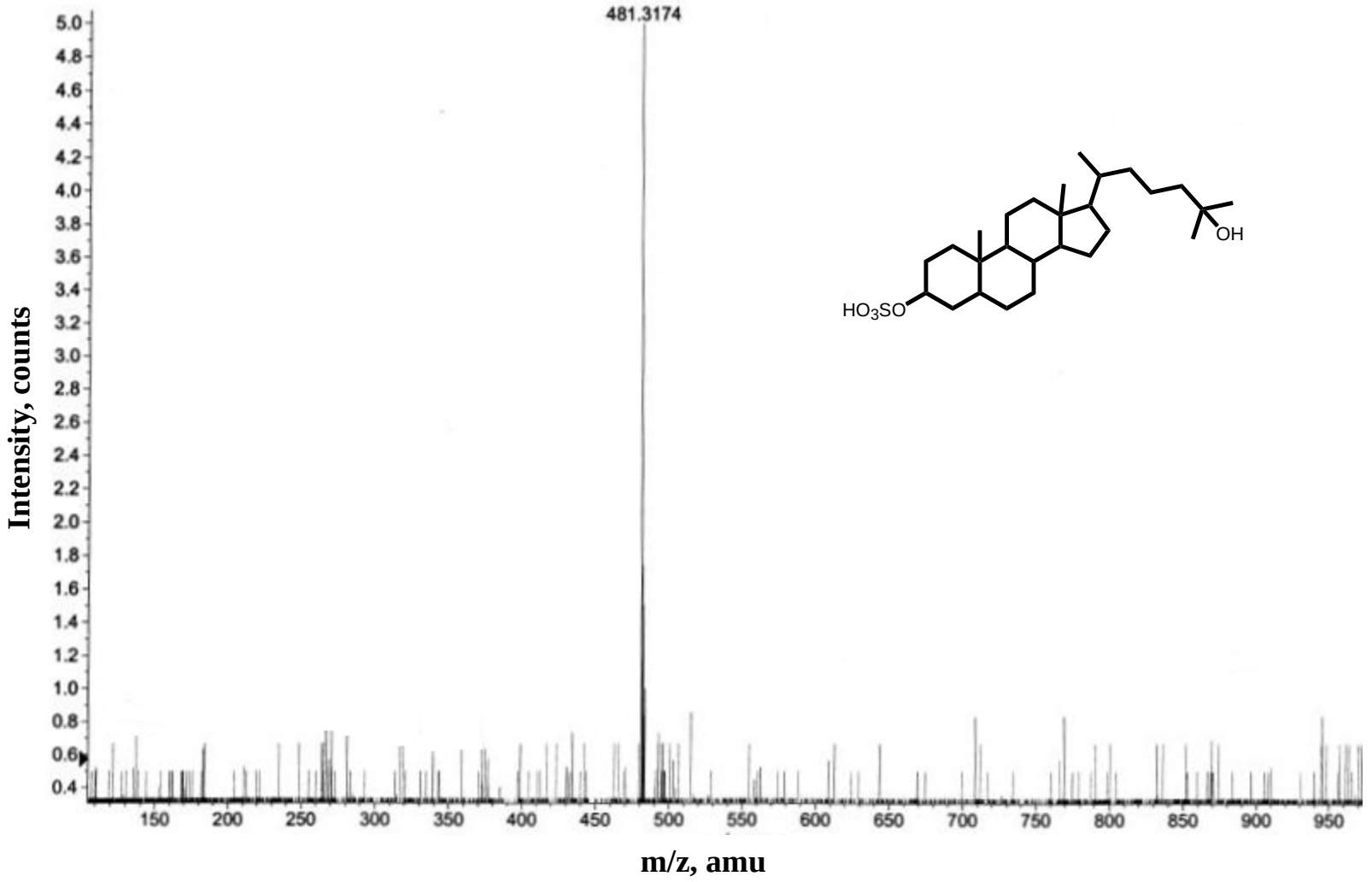

Supplementary Figure 2